

Spring 2019

Analysis of Cellular Interactions Within a Collagen Hydrogel

Austin N. Worden

Follow this and additional works at: <https://scholarcommons.sc.edu/etd>



Part of the [Biomedical Engineering and Bioengineering Commons](#)

Recommended Citation

Worden, A. N.(2019). *Analysis of Cellular Interactions Within a Collagen Hydrogel*. (Master's thesis). Retrieved from <https://scholarcommons.sc.edu/etd/5165>

This Open Access Thesis is brought to you by Scholar Commons. It has been accepted for inclusion in Theses and Dissertations by an authorized administrator of Scholar Commons. For more information, please contact digres@mailbox.sc.edu.

Analysis of Cellular Interactions Within a Collagen Hydrogel

by

Austin N. Worden

Bachelor of Science

University of South Carolina-Aiken, 2016

Submitted in Partial Fulfillment of the Requirements

For the Degree of Master of Science in

Biomedical Science

School of Medicine

University of South Carolina

2019

Accepted by:

Jay D. Potts, Director of Thesis

Robert L. Price, Reader

Ioulia Chatzistamou, Reader

Cheryl L. Addy, Vice Provost and Dean of the Graduate School

©Copyright by Austin N. Worden, 2019
All Rights Reserved.

ACKNOWLEDGEMENTS

I would like to give the utmost thanks to my mentors, friends, and family, especially my parents and grandparents. Without your support, guidance, and encouragement, none of this would have been possible.

ABSTRACT

Evidence has arisen over the past several years that use of a three-dimensional (3D) culture system provides a distinct advantage over two-dimensional (2D) systems when cellular interactions are examined in a more natural environment. Changes in morphology, speed, and directionality of cells tested in both planar and 3D matrices have all demonstrated that using 3D system is advantageous. The changes to the cellular migration patterns were shown to be dependent on several variables within the surrounding substrate including cellular content, physical environment, and the matrix chemical milieu. We have taken advantage of using collagen hydrogels as a 3D scaffold for culturing cells for an extended period of time which has led to intriguing discoveries. One such discovery is that independent of cell type, cells which were placed on top of the hydrogel formed a ring structure we termed a toroid. These toroids take the shape of the well in which they are cultured. These toroidal cells appear long, thin, and are reminiscent of spokes on a wheel. However, when cells were mixed into the collagen hydrogel, a gel contraction was observed, but the cells remained homogenous throughout and no toroid was formed. In our studies, stem cells, lens epithelial cells, cardiac fibroblasts, microvascular endothelial cells, and cancer cells, were used individually or in combination. Cells were placed on the top of collagen hydrogels to observe their behavior in this new multicellular environment. We observed that when the different cell types

were mixed together they formed a tighter toroid than normal. We also investigated the movement of cells during the toroid formation. To that end, $\beta 1$ integrin, a member of the integrin family of membrane receptors important for cellular adhesion and recognition, was overexpressed in cells using a plasmid tagged with Green Fluorescent Protein (GFP). We were successful at expressing GFP tagged $\beta 1$ integrin in cells and observing them in the collagen matrix. Our observations will contribute to the understanding of toroid formation and form the foundation of future computational modeling experiments examining cellular behaviors in response to different microenvironments.

TABLE OF CONTENTS

Acknowledgements.....	iii
Abstract.....	iv
List of Figures	vii
List of Abbreviations.....	viii
Chapter 1: Introduction	1
Chapter 2: Methods	11
Chapter 3: Results	20
Chapter 4: Discussion.....	35
Chapter 5: Future Directions.....	38
References	40

LIST OF FIGURES

Figure 1.1 Cell appearance during toroid formation	8
Figure 1.2 Spheroid filled with FITC shows no leakage	9
Figure 1.3 Cellular remodeling of the collagen gel	10
Figure 2.1 Restriction digest check of ITGB1 expression vector	19
Figure 2.2 Comparison of on-top and mixed in hydrogels.....	19
Figure 3.1 Bar Graph analysis of collagen concentration series	26
Figure 3.2 Collagen concentration series.....	27
Figure 3.3 VitroGel™ 3D comparison to animal matrices	28
Figure 3.4 Bright-field time series	29
Figure 3.5 Fluorescent time series.....	30
Figure 3.6 40X objective view of ITGB1 expression in ADSCs	31
Figure 3.7 63X oil objective view of ITGB1 expression in ADSCs	32
Figure 3.8 ADSC and BMSC mixed cells on a dish	33
Figure 3.9 NHF and ARPE mixed cell toroid.....	34

LIST OF ABBREVIATIONS

AmphoB.....	Amphotericin B
BSA.....	Bovine serum albumin
DAPI	4',6-diamidino-2-phenylindole
DMEM.....	Dulbecco's Modified Eagle Medium
EDTA	Ethylenediaminetetraacetic acid
FBS.....	Fetal Bovine Serum
HEPES.....	4-(2-hydroxyethyl)-1-piperazineethanesulfonic acid
MEM	Minimum Essential Media
PBS.....	Phosphate Buffered Saline (pH 7.4)
P/S.....	Penicillin Strip
RPM.....	Revolutions Per Minute
TAE.....	Tris-Acetate-EDTA

CHAPTER 1

INTRODUCTION

1.1 Background

Over the last two decades, traditional two-dimensional (2D) techniques for cell culture have seen the need for improvement. While these techniques are still in use in laboratories, a new-aged three-dimensional (3D) cell culture is rapidly advancing as the go to technique due to its consistency with micro-environments such as the cellular milieu and extracellular matrix (ECM). Advantages for using a 3D cell culture system far surpass those of a traditional 2D culture by providing more accurate physiological responses such as vascular lumen formation, changes in the expression of RNA and proteins, increased differentiation, reduced proliferation, and in vivo tissue development (van Duinen et al, 2015). While the transition to a more physiological-like tissue model is important for scientific advancement, 3D techniques are still imperfect because of their inability to fully provide the complexities of multicellular tissues, complete lack of a vascular network, incapability of precise gradient control, and inconsistency in media exchange. Throughout the first several years of developing these 3D culture systems, attempts to create a porous scaffold took scientists on a journey using solvent casting, particulate matter leaching, gas foaming, separation of phases, molding melted substances, and freeze-drying (Mir and Nakamura,

2017). While these attempts had their successes and failures, new materials and technology have been found to create a more accurate micro-environment. The use of hydrogels and 3D bioprinting have emerged to provide a simple solution to porous scaffolds. Hydrogels have a range of uses from cell storage and culture to the observation of cell-cell interactions and ability to control the orientation of single cells. These hydrogels are dynamic in their possibilities (Stanton et al, 2015). One such combination of the two is a more recently designed “bioink” where hydrogel is 3D printed. In a paper by Stanton et al (2015), these bioinks were composed of a liquid gel containing cellular suspension that was printed into a scaffold. Once the printing process was finished, the newly constructed and polymerized hydrogel created a physical scaffold for the internal cells which were seen to have a normal viability and organelle activity when observed with a fluorescent live/dead assay and high-resolution imaging. These hydrogels were then shown to be biodegradable using protease and nucleases thus allowing them to have an application in medicine as a temporary scaffold (van Duinen et al, 2015). The term hydrogel refers to gel that contains over 90% water and polymer chain networks which are hydrophilic. These polymer chains are bound together through cross-linking thus creating a three-dimensional (3D) solid. This allows for a high structural integrity, absorbency, and flexibility in the presence water and other biomaterials (Hesse et al, 2010).

Hydrogels can be used in a wide variety of ways including for tissue repair and engineering, coated wells for cell culture, drug delivery, and 3D matrices for modeling and imaging (Antoine et al, 2015). Due to their biocompatibility and

widely tunable structure, they have been shown to simulate the extracellular matrix (ECM) in physical structure to a point that promotes cell proliferation and regeneration of tissues. In some studies, hydrogels have been capable of encapsulating various drugs for delivery (Mao et al, 2019; Oliveira et al, 2015). Other studies have focused on the use of the hydrogel as a matrix in which cells can be suspended and observed for interactions (Mao et al, 2019). While there have been several different hydrogels created with natural and synthetic materials such as agarose, fibrin, and silk to name a few, the most widely used polymer is collagen which is an important component in the ECM of tissues like skin, bone, cartilage, ligament, and tendon (Hesse et al, 2010). Other advantages of using collagen hydrogels include a straightforward preparation, cells can be placed directly on the surface or mixed in, and the translucent gels allow for immunolabeling and imaging (Gourdie et al, 2012).

Collagen is widely used due to its abundance in most organisms and it is recognized by cells that allow for cell adhesion, proliferation, migration, differentiation, and degradation (Hesse et al, 2010). Collagen hydrogels, created from native tissues, are used regularly as a cell culture scaffold as well as in tissue engineering. As previously stated, the similarity of structure to the natural ECM environment creates a major draw to using collagen hydrogels, however, it must be greatly optimized for solubilization, solution components, pH, collagen concentration and polymerization temperature in order to produce better results than synthetic ECM. When properly optimized, collagen hydrogels can better replicate the properties and physiological cues of the target tissues while

mimicking cellular functions such as nutrient diffusion and growth factors. (Antoine et al, 2015).

Our lab has been using collagen and hydrogels for an extensive period of time. We have used collagen gels to mimic early cardiovascular development (Runyan et al, 1992). We have also created a collagen bioassay to study cardiac muscle development (Potts and Runyan, 1989). Recently, we have used collagen hydrogels to examine the self-organizing structure of cells (Gourdie et al, 2012). What we observed was quite unique. When cells were placed on top of the hydrogel, a toroid ring of cells was formed. These toroidal cells appeared long and thin during migration from the outer gel to the middle looking like the spokes of a wheel. However, when the cells were mixed inside the hydrogel, contraction of the scaffold was observed, but the cells remained spread throughout (Figure 1.1).

1.2 Previous Studies

Advanced testing for this phenomenon included numerous cell types such as stem cells, lens epithelial cells, cardiac fibroblasts, microvascular endothelial cells, and cancer cells either mixed in or placed on top of the matrix (Table 1.1). With the exception of cancer cells, toroids were formed when cells were placed on top of the matrix. No toroids were formed when any cell types were mixed into the matrix.

Table 1.1 Cell types tested for toroid formation when placed on top of different matrices.

	Collagen I	Collagen III	VitroGel 3D	Study
NHF	Yes	Yes	No	This Study
ARPE-19	Yes	Yes	No	This Study
BMSC	Yes	Yes	No	This Study
ADSC	Yes	Yes	X	This Study
Cancer Cells	No	X	X	Previous Lab Study
NHF + ARPE-19	Yes	X	X	This Study
NHF + BMSC	Yes	X	X	This Study
NHF + ADSC	Yes	X	X	This Study
ARPE-19 + BMSC	Yes	X	X	This Study
ARPE-19 + ADSC	Yes	X	X	This Study
BMSC + ADSC	Yes	X	X	This Study

In addition to numerous cell types and different matrices; the size and shape of the well and type of hydrogel matrix were also tested. Regarding the shape and size of the well, toroids formed to 45% of the well diameter, meaning the toroids were larger or smaller depending on the size of the well. The toroids also form in reaction to the shape of the well. No matter what shaped well it was placed (i.e. square, rectangle, or triangle), the toroid would form to that shape. However, when observed in a square well for more than twenty-four hours, a new phenomenon was discovered-the creation of a spheroid. These spheroids were circular, 3D structures that were sealed completely except for a hole at the top. They were also shown to be hollow and when a fluid was inserted inside the spheroid, it showed no leakage (Figure 1.1). Hydrogel matrices were also changed to determine if toroids were formed. Previously, type I collagen was

tested. In addition, type III collagen, a non-animal hydrogel named VitroGel™ 3D, and a combination of collagen types I and III have been tested. The type III collagen also created toroids while the VitroGel™ 3D produced cellular clumps as advertised by the company.

Another aspect that was studied in our lab was the remodeling of matrix by the cells. To test this, 4T1 cancer cells and BMSCs were placed on top and inside collagen gels and allowed to incubate for 24-hours. These gels were then taken and weighed to determine the amount of matrix remodel. The weight of the gel correlated with the amount of gel being degraded and remodeled by the cells. The gels with BMSC cells mixed in showed greater remodeling than the gels with BMSC placed on top (Figure 1.3 D). The cancer cells showed little to no difference in weight when the on top and mixed in were compared (Figure 1.3 C). However, when the cancer cell and BMSC remodeling were compared, the BMSC showed greater remodeling (Figure 1.3 A and B).

Members of the integrin family are membrane receptors that are important in cellular adhesion and recognition (Iervolino et al. 2018). Processes that use the integrin family members include hemostasis, tissue repair, and immune response. These integrins provide links and transmit signal transduction between the actin cytoskeleton and ECM. The sub-class, β -integrins, are responsible primarily for connecting integrin dimers to subcellular regions such as focal adhesions (Sun et al, 2018). Integrin $\beta 1$ (ITGB1) is a cell surface receptor encoded by the *ITGB1* gene in humans. The main function of $\beta 1$ integrin is as a collagen receptor when ITGB1 forms a complex with integrins $\alpha 1$ and 2. We

sought to overexpress and visualize $\beta 1$ integrin in cells using an expression plasmid that contains the ITGB1 expression cassette coupled to a Green Fluorescent Protein (GFP) tag (Iervolino et al. 2018; Zhang et al, 2018).

1.2 Objective, Hypothesis, and Aims

The *objective* of this study was to observe and image cellular behavior when placed on top and mixed into the collagen hydrogels in addition to studying cell-to-cell interactions when multiple cell types were mixed and seeded on collagen hydrogels. We used collagen type-I hydrogels because previous studies in our lab have shown consistent cellular toroid formation for all non-cancerous cell types. To that end, we chose to use mouse Neonatal Heart Fibroblast (NHF), human Retinal Pigment Epithelial cells (ARPE-19), mouse Adipose-derived Stem Cells (ADSC) and mouse Bone Marrow Stromal Cells (BMSC) to provide a broad spectrum of cell lineages.

We *hypothesized* that all mixed cells would interact and migrate together instead of two separate entities and that by observing these interactions using labeled integrin receptors, we can map migration patterns through the hydrogel thus gaining insight into how the different cell types arrange themselves when competing for resources. This should provide the unique opportunity to characterize the cellular response in different microenvironments that could aid in the development of new biomaterials that communicate and interact with cells, thus creating the possibility to make significant steps toward the advancement of bioactive materials and cellular responses.

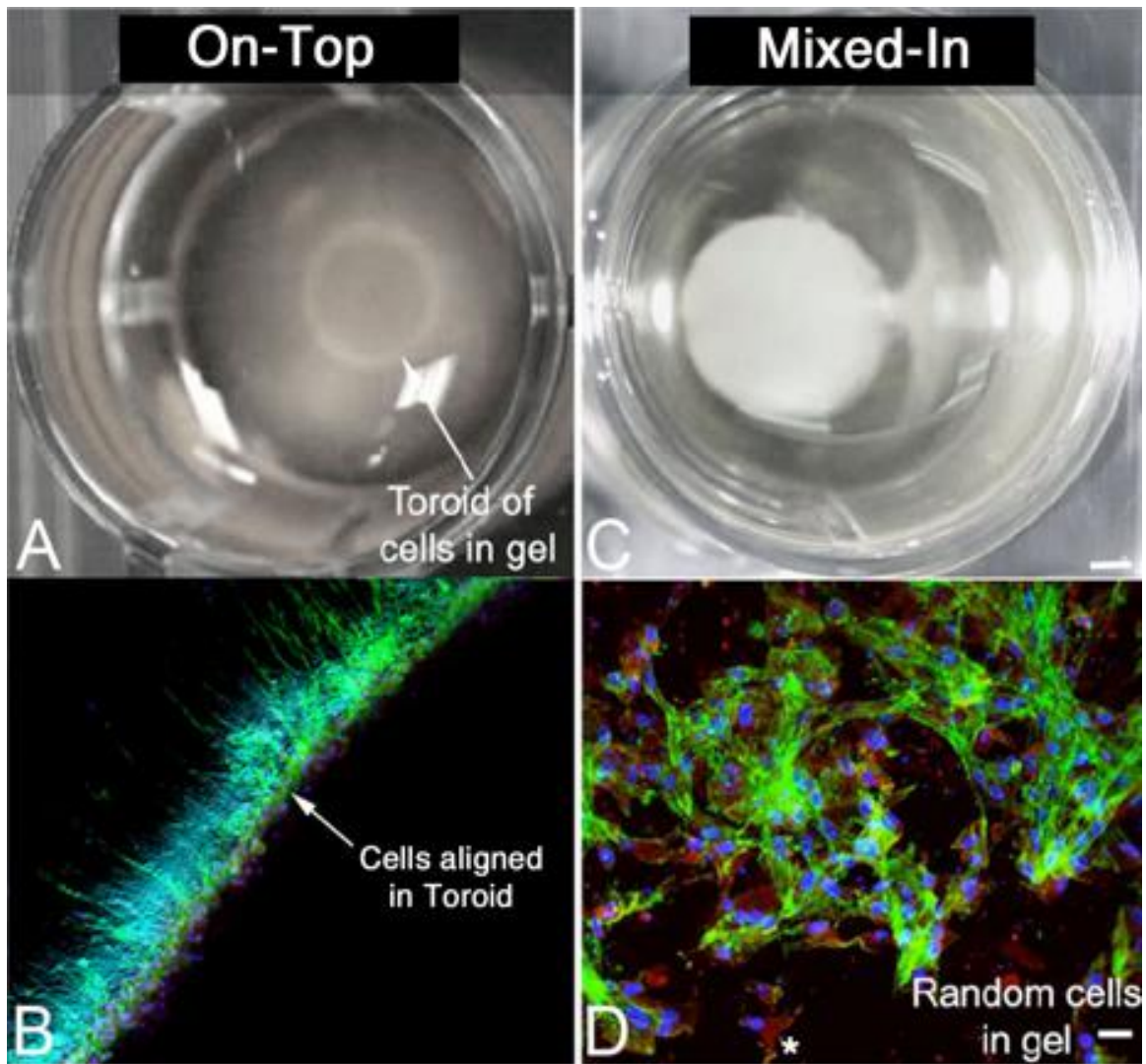


Figure 1.1 Cell appearance during toroid formation. A toroid is formed when cells are placed on top of a hydrogel (A). These toroidal cells are long, thin, and look like the spokes of a wheel during migration (B). However, when cells are mixed into the hydrogel, contraction of the scaffold was observed (C), but the cells remained spread throughout the gel in a random fashion (D).

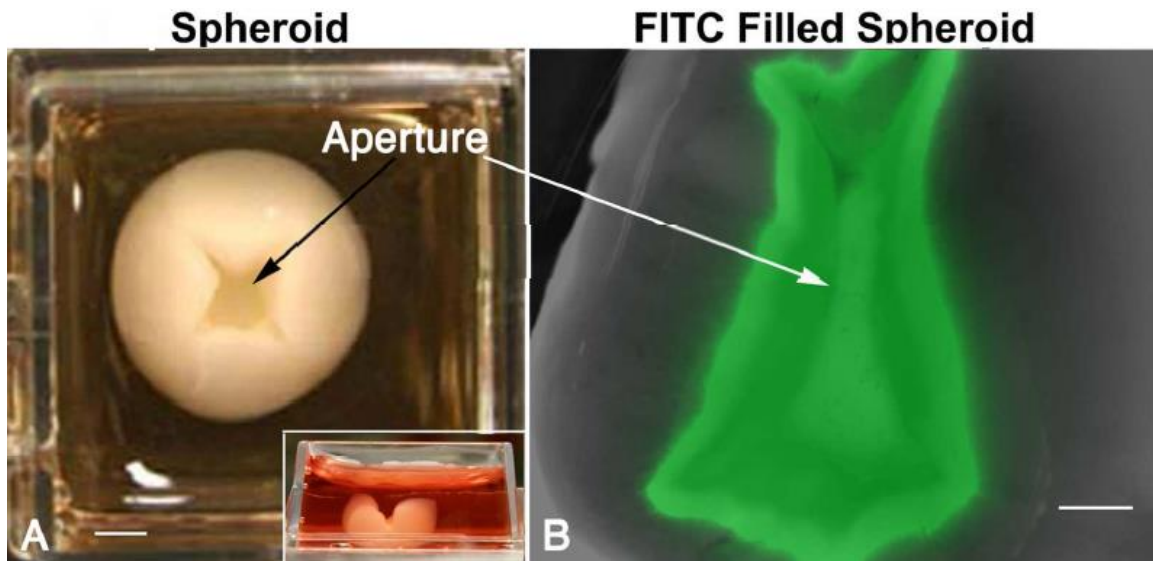


Figure 1.2 Spheroid filled with FITC shows no leakage. Spheroids are circular, 3D structures that are sealed completely except for a hole at the top and seemingly hollow. When a fluid was inserted inside the spheroid, it showed no leakage.

Cellular remodeling of the Collagen gel₁

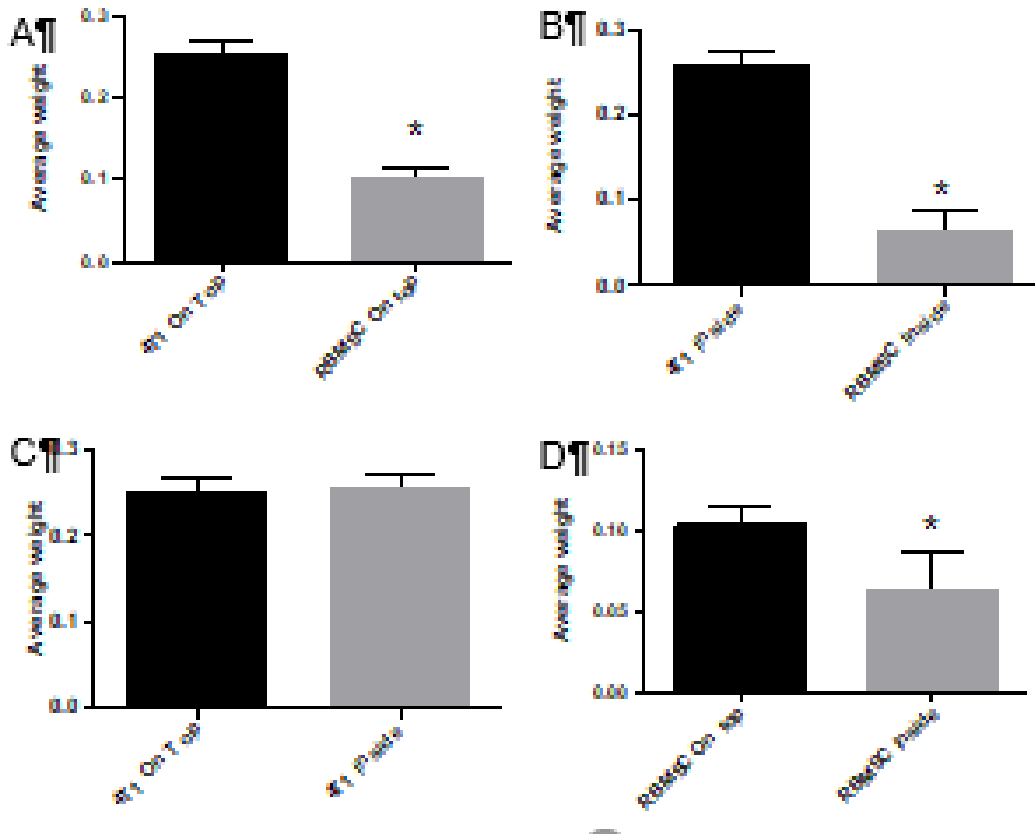


Figure 1.3 Cellular remodeling of the collagen gel. A) Comparison of 4T1 cancer cells on top and rat bone marrow stem cells (RBMSC) on top. RBMSC showed greater remodeling by weighing less. B) Comparison of 4T1 mixed in and RBMSC mixed in. The RBMSC showed greater remodeling. C) Comparison of 4T1 mixed in and on top. There is little to no difference in weight suggesting neither contained much remodeling. D) Comparison of RBMSC mixed in and on top. Both showed the effects of remodeling, however the mixed in showed greater remodeling effects.

CHAPTER 2

METHODS

Mouse Neonatal Heart Fibroblast (NHF), human Retinal Pigment Epithelial cells (ARPE-19), mouse Adipose-derived Stem Cells (ADSC) and mouse Bone Marrow Stromal Cells (BMSC) were obtained, cultured, stained, placed in or on top of hydrogels, and imaged. Images were collected and analyzed using several different pieces of equipment.

2.1 Specimen Preparation

All cells were cultured in DMEM with 10% FBS, P/S, and AmphoB. Upon passaging the cells, the media and 0.25% Trypsin/ EDTA were pre-warmed to 37°C. Old cell media was removed from the flask or dish. Two milliliters (mL) of the 0.25% Trypsin/EDTA was added and allowed to remain on the cells for approximately 3 minutes at room temperature. This caused the cells to become detached from the culture flask. The flask was then tapped to ensure all cells were detached and viewed under the microscope for confirmation. The cell/trypsin mixture was then removed from the vessel and placed in a 15 mL conical tube with 10 mL of fresh media to inactivate the trypsin. This tube was spun down in a centrifuge at room temperature, 800 rpm, for 8 minutes. When finished, the supernatant was aspirated, and the remaining cells were resuspended in fresh media and added to the new culture flask.

2.2 Cell Staining

To image the cells within the gel and toroid, a series of antibodies and stains were used. The stains included DAPI, Phalloidin 488, Vybrant Multicolor Cell-Labeling Assay, and a Beta-1 Integrin expression vector. DAPI, or 4',6-diamidino-2-phenylindole, is a nuclear stain that binds to adenine-thymine rich areas within DNA. Upon binding to DNA, it has a maximum emission at 461 nm which is in the blue spectrum. Phalloidin is a phallotoxin that is found in the death cap mushroom. Derivatives of this toxin are usually fluorescently tagged and tightly binds to filamentous actin (f-actin) within a cell. To label the f-actin, we used primarily Phalloidin 488 which is a green-fluorescent dye that emits light at 518 nm. Another important stain used was the Vybrant Multicolor Cell Labeling Kit which contain three stains DiO (501 nm), DiL (565 nm), and DiD (665 nm) that binds to the cellular membranes using built-in molecular probes. These dyes can be added straight to cell culture media to stain the entirety of a cell. This is an important tool when studying cell-cell interaction, adhesion, or migration. The final tool was the aforementioned expression vector containing a fluorescent tag (van Gaalen, 2010; Renz 2013).

2.21 Antibody Staining

When staining cells, it is necessary to use antibodies when looking for a specific protein, the following antibody staining protocol can be used when staining with DAPI and Phalloidin 488 as well. To stain cells within the toroid, the cells were fixed with 2% Paraformaldehyde (PFA) (pH 7.2) and rinsed with PBS. They were permeabilized using 0.1% Triton X-100/ 0.01M Glycine/ PBS for 30

minutes. To stop permeabilization, the cells were washed 3 times for 5 minutes each in PBS. Cells were then blocked in 5% BSA for 30 minutes before another wash cycle in PBS. In our staining we used our 1^o mouse monoclonal R26.4C (Zo1) antibody from Developmental Studies Hybridoma Bank (DSHB) diluted 1:200 in PBS and applied overnight at 4°C. The following day, the primary antibody was washed off with PBS. The secondary antibody, Invitrogen Alexa Fluor 546 donkey anti-mouse IgG, was diluted 1:250 in PBS and applied for 1 hour in the dark at 37°C. Another wash cycle was performed with PBS. If antibodies are not being used, then the protocol can skip to the final stage where DAPI (diluted 1:1000 in PBS) and Phalloidin 488 (diluted 1:200 in PBS) are applied in the dark either for 1 hour at room temperature or overnight at 4°C. The cells were then washed once more to remove any residual staining materials and imaged on the EVOS FL Auto and the Zeiss LSM 510 confocal microscope.

2.22 Vybrant Multicolor Cell Labeling Kit

The Vybrant multicolor cell labeling kit from ThermoFisher Scientific contains three stains DiO (501 nm), DiL (565 nm), and DiD (665 nm) which can be added straight to cell culture media to stain cell membranes using a built-in molecular probe as a dye delivery system. While cells were suspended in media, 5 microliters (µL) of one of the stains was added and mixed in by gentle pipetting. The suspension was then incubated at 37°C for 15 to 20 minutes before being centrifuged at 1500 rpm for 5 minutes. Supernatant was aspirated and the cells were gently resuspended in fresh media. This centrifugation and resuspension steps were repeated 2 more times before a 10-minute recovery time for the cells.

These cells could then be used or observed as they were imaged on the EVOS FL Auto and the Zeiss LSM 510 confocal microscope.

2.3 Transfection Assay

Transfection is the introduction of novel genetic material into a cellular host. The β 1 integrin was chosen due to its proficiency in collagen binding. The β 1 integrin (ITGB1) human expression vector was purchased from OriGene (Rockville, MD). It first had to be tested using a restriction digest and gel electrophoresis to determine if the vector was correct. A restriction digest was performed using 5 μ L of the vector, 2 μ L 10x NEBuffer Cutsmart, 1 μ L HindIII restriction enzyme, and 12 μ L nanopore water. This was incubated for 1 hour at 37°C followed by an immediate transfer to 65°C for 15 minutes in order to stop the digest. Next, 5 μ L of loading dye was added to prepare for the gel electrophoresis. A 1.25g agarose in 50 mL 1X TAE buffer gel was created with 10 μ L Ethidium Bromide. Once the gel was polymerized, a 1 kilobase DNA ladder was added to lane 1, an undigested vector in lane 2, and 2 identical vector restriction digests followed. To ensure proper separation, this was run at 120 volts for 30 minutes (Figure 2.1)

Once this was observed to be correct, the ITGB1 vector could then be transfected into cells using the Invitrogen Lipofectamine RNAiMAX Reagent. Cells were grown to 60-80% confluent at the time of transfection. Two microliters of the Lipofectamine RNAiMAX Reagent was diluted in 25 μ L Opti-MEM media. One microliter of the ITGB1 vector was diluted in 25 μ L Opti-MEM media. The two dilutions were added together at a 1:1 ratio and allowed to incubate at room

temperature for 5 minutes. This mixture was then added to the cells in a drop-wise fashion and incubated at 37°C for 24 hours before being visualized on the EVOS FL Auto and the Zeiss LSM 510 confocal microscope.

2.4 Hydrogel Formation

To create the collagen hydrogel, we started with an 8:1:1 ratio of type-1 collagen, HEPES, and MEM. To begin, we mixed 100 μ L each of HEPES and MEM first in a tube and then added 800 μ L Collagen I to the tube and mixed thoroughly so that no separation was observed and kept on ice. This was to make 1 mL of hydrogel matrix. Next, 100 μ L of the hydrogel mix was pipetted into a 96-well plate. This well plate was then incubated at 37°C for 1 hour, or until the gels were solidified properly. During this stabilization phase, the desired cells were passaged to the point before placing them into a new culture flask and, if the Vybrant Cell Labeling Assay was used, this was the point at which cells were added to the labeling mix. Once the gels were polymerized, 50 to 100,000 cells were placed on top of the gels using approximately 100 μ L of media. This was incubated at 37°C for 30 minutes. After this incubation step, the gels were released from the sides of the wells with a thin-tipped probe and the well was topped off with fresh media. The final incubation was at 37°C for 24 hours.

Collagen I has been universally accepted as a prominent matrix component when creating hydrogels. In our previous studies, both collagen I and collagen III were proven successful at producing toroids, however, to the naked eye, collagen III seemed to create smaller, more compact rings. To test this observation, a collagen concentration series was performed in triplicate using

different concentrations of collagen I and collagen III. These hydrogels still followed the 8:1:1 ratio as stated before, however the concentrations of the 800 μL collagen I was diluted with collagen III. These concentrations were 100% collagen I (800 μL collagen I), 80:20 (640 μL collagen I: 160 μL collagen III), 60:40 (480 μL collagen I: 320 μL collagen III), 60:40 (320 μL collagen I: 480 μL collagen III), and 100% collagen III (800 μL collagen III). Neonatal heart fibroblasts in media were placed on top of the gels and incubated for 24 hours at 37°C. The gels were then imaged on the EVOS FL Auto and toroid diameters were measured and averaged.

In order to make the hydrogels containing multiple cell types, the same process was used, however, cell media was mixed into the hydrogel matrix. One-hundred microliters (containing 25,000 cells of each type) of this new mixed-in matrix was pipetted into the 96-well plate and allowed to incubate at 37°C for 24 hours.

Upon completion of the 24-hour incubation period, toroids were visible to the naked eye in the wells where cells in media were placed on top of the hydrogel in contrast to the mixed-in gels which had slight contraction, but no toroid was formed (Figure 2.2). At this point, the excess media was aspirated, the hydrogels were rinsed with PBS, and then fixed with 2% Paraformaldehyde for 30 minutes at room temperature. Following fixation, the gels were rinsed another two times in PBS and then stored at 4°C until antibody addition.

2.5 VitroGel™ Formation

While toroids universally form using collagen matrix, we set out to test whether the same toroid formation would happen in a non-animal model. The hydrogel model that was used was VitroGel™ 3D from The Well Bioscience. This is a non-animal, polysaccharide system described to closely mimic a natural extracellular matrix environment by simply mixing the hydrogel solution and culture media containing 50,000 NHF cells. To create the VitroGel hydrogel with cells inside, the 3D solution and culture medium was warmed to 37°C. A 1:3 dilution of hydrogel solution to deionized water was created before mixing one part of this dilution with one-part cell culture medium. This was mixed gently with a pipette before adding 100 µL to each well in a 96-well plate. This was incubated for 15 minutes before adding fresh media over top.

To create a hydrogel with cells placed on top, one part of the previous 1:3 dilution was mixed with one-part fresh culture media and mixed gently. One-hundred microliters were placed in the desired number of wells of a 96-well plate and allowed to incubate at 37°C for 30 minutes. Once polymerized, 100 µL of cell containing media was placed over top and incubated at 37°C for 24 hours. After the 24-hour incubation, both the inside (50,000 cells mixed into the hydrogel) and the on-top (50,000 cells in media placed over top the hydrogel) gels were stained with the desired antibody or labels.

2.6 Toroid Imaging

To observe and image the toroids, a number of microscopes were used. The Nikon Eclipse TS100 was used for initial viewing of the toroid. If it were determined that a toroid formed, we next used the Invitrogen EVOS FL Auto Live Cell Imaging System. This machine is fully-automated to allow for live cell time-lapse and multi-well imaging as well as image stitching. While the EVOS was used for much of the toroid imaging, other images were needed for depth and higher resolution. To achieve this, we used the Zeiss LSM 510 META Confocal Scanning Laser Microscope and the Leica SP8 TCS Multiphoton Confocal. The two confocal systems offer a wide array of objectives that allow for deep imaging as well as second harmonic collagen imaging.

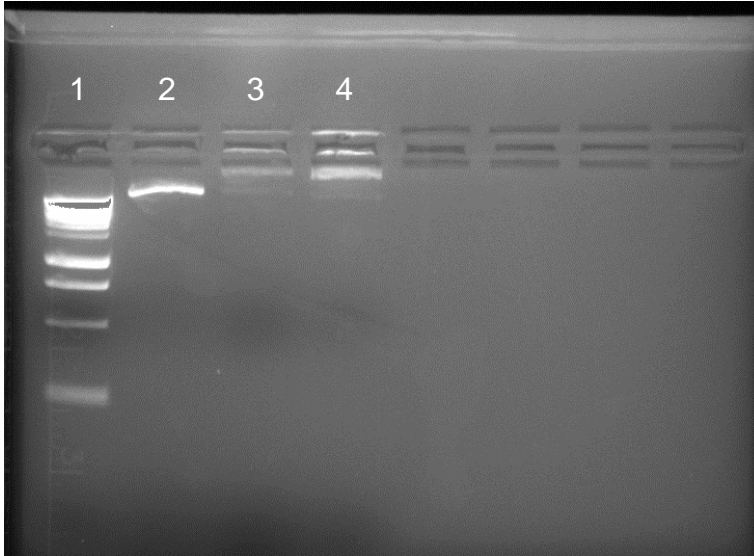


Figure 2.1 Restriction digest check of ITGB1 expression vector. Lane 1 shows the 1 kb DNA ladder. The expression vector was 8,954 base pairs(bp) which was seen in lane 2 at approximately 9,000 bp. In lanes 3 and 4, the digested vector was split into pieces (5,672 bp, 3,282 bp, and 2,390 bp) and can be seen to be successful.

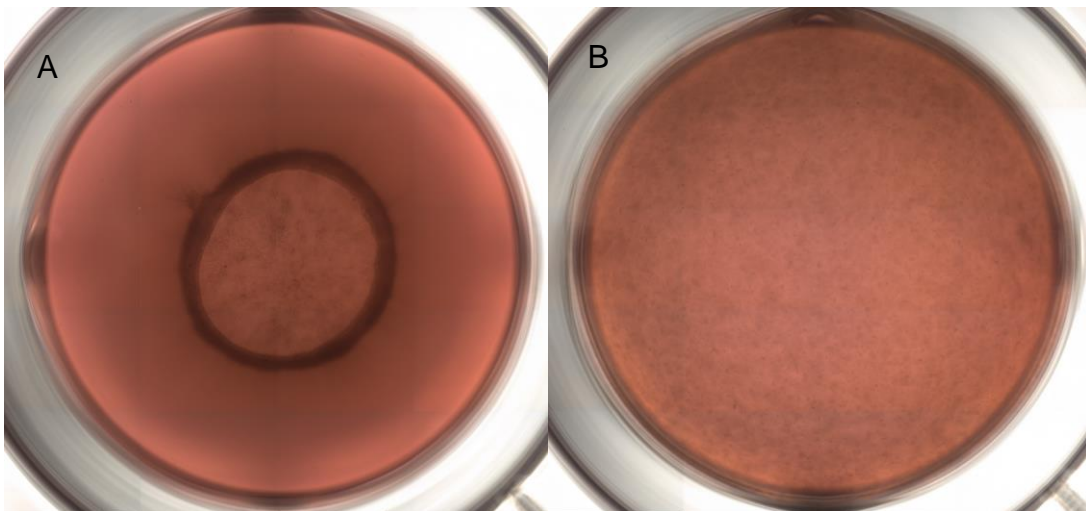


Figure 2.2 Comparison of on-top and mixed in hydrogels. A) The result of a hydrogel with NHF cells in media placed on-top, a toroid. B) The result of NHF cells in media being mixed into the hydrogel matrix, no toroid.

CHAPTER 3

RESULTS

3.1 Collagen Hydrogel Testing

To test the observation that toroids formed using collagen III hydrogels were smaller and more compact than those formed in collagen I hydrogels, and to determine whether a single collagen, collagen type I, or a combination of collagen provided a more *in vivo*-like environment for our studies, a collagen concentration series was performed in triplicate using concentrations of 100% type I, 80:20, 60:40, 40:60, and 100% type III. Fifty-thousand Neonatal Heart Fibroblasts (NHF) were used as the cell type for producing toroids and a 96-well plate was used to achieve maximum data while still producing the desired toroid. After a 24-hour incubation at 37°C, the size of the toroid was measured using the EVOS FL Auto and the three toroid measurements were obtained for each concentration and then averaged.

As seen in Table 3.1, Figure 3.1 and Figure 3.2, toroid formation progressively grew smaller with increasing collagen type III. The toroids that were created out of 100% collagen I maintained an average size of 2,700 μm while the toroids of 100% collagen III averaged 1,700 μm creating a statistically significant 37.04% difference between 100% collagen I and 100% collagen III. The p-value

between the 100% collagen 1 and 100% collagen III was .000066 which was significant at $p < .01$.

Table 3.1 Collagen Concentration Series

Percent Collagen I	Percent Collagen III	Avg Size of Toroid (μm)	% Difference from Col I
100	0	2700	0.00%
80	20	2500	7.41%
60	40	2200	18.52%
40	60	2000	25.93%
0	100	1700	37.04%

3.2 VitroGel™ 3D Testing

To date, all of the toroids created with all the various gel types were created using collagen hydrogels. To test whether the non-animal model, VitroGel™ 3D, would initiate the same reaction as our collagen matrices, NHF and human Retinal Pigment Epithelial (ARPE-19) cells were mixed-in and placed on-top using the VitroGel manufactured protocol. In a minimum of 10 replicates, VitroGel matrices were seeded and all the results from the on-top were similar in that toroids did not form using this non-animal matrix. When analyzing the on top hydrogels, cells formed clumps (Figure 3.3A). Figures 3.3B and 3.3C show these resulting NHF cell clumps stained with DAPI and Phalloidin 488. Nuclei (blue) are clearly clumped together with the f-actin (green) surrounding the clump. These

cell clumps are identical to the images that the company uses for its advertisement.

3.3 Time Series Mapping

While much of the imaging of the toroids in their final ring-like structure was at approximately 24 hours, there is very little data on the time during the process the cells take to form a toroid. To address this issue, a time lapse of the formation of the toroid was performed using the EVOS FL Auto. In Figure 3.4, four frames of a time series movie are shown. This toroid was formed using a collagen type I hydrogel and NHF in a 96-well plate. Image A shows the surface of the hydrogel with cells spread throughout the gel after the first hour. There is little documentable movement over the next several hours until the 10th hour in image B. The cells are shown to have condensed greatly from the first hour into a toroid-link structure. These cells continue to remodel and migrate within the collagen hydrogel by hour 16 (image C) until they reach their final spot at the 24th hour time point (image D). One issue with this time lapse approach is that using bright-field time lapse it is very difficult to see individual cells moving over the 24-hour time period.

To address this problem, we again performed a time lapse series but used fluorescently labeled cells. This was set up the exact same way as the bright-field time series with the 100% collagen I and using a 96-well plate, however the NHF cells were stained using the Vybrant Cell Labeling Kit with the DiD stain that emits at 665 nm (or in the far-red spectrum). Since this kit labels the cell in its entirety, each red dot in Figure 3.5 can be considered a cell. Like in the previous

figure, still frames were taken at the 1, 10, 16, and 24-hour marks (A-D respectively). Here, we see the same results as the bright-field time series where cells collectively move from diffused in the well to a tight ring-like toroid, however, this allows us to visualize and map individual cells as they move towards the toroid. This is key to determining how the cells migrate through the matrix and how they interact with surrounding cells.

To further investigate how the cells migrate over time, studies have begun in which gels were fixed at a specific time in order to observe the cell to cell contact using Zo1 and Connexin 43 antibodies and the cell to matrix interactions using focal adhesion kinase and β 1 integrin. To date, we have not observed the cellular labeling that is characteristic for these antibodies due to improper labeling of the cells.

3.4 Integrin beta-1 Expression in Adipose Derived Stem Cells

Studies on stem cells have been increasing in countless biological areas. We too have focused on a newer type of stem cell, adipose derived stem cells (ADSC) due to their numerous advantages in regenerative medicine such as their capacity for multipotential differentiation and self-renewal. As previously stated, integrin beta-1 (ITGB1) is a member of the integrin family of ECM receptors that are key membrane receptors for cellular adhesion and recognition and are integral in processes such as hemostasis, tissue repair, and immune response.

To begin to examine how these ADSCs migrate to form toroids, an expression vector containing an ITGB1 cassette was transfected into ADSCs so that the cell-to-ECM connections could be seen and imaged using confocal microscopy. When successfully transfected, integrin β 1 receptors fluoresced green due to the Green Fluorescent Protein (GFP) tag that had been previously inserted into the vector. In Figures 3.6 and 3.7, images at 40X and 63X, respectively, show expression of the β 1 protein in ADSCs with a bright green fluorescence and the nuclei of each cell counterstained blue with DAPI. These results suggest that the β 1 integrin is expressed on the surface that mimics the underlying f-actin inside the cells. The β 1 also clusters in a perinuclear fashion and is abundantly expressed throughout the cell. This is an important result as studies on connections between the cells and the collagen hydrogel is of extreme importance to our studies.

3.5 Mixed Cell Interactions

The previous studies have looked at effects of the collagen hydrogel composition and the cellular response at distinct time points during toroid formation. We have created a process to express collagen binding receptor on the cells and watch their movement during toroid formation. These studies were performed to ask specific questions of a specific type of cell during toroid formation. We next extended these studies to include multiple cell types mixed together during the formation of the toroid. A mixture of 25,000 ADSCs and 25,000 BMSCs were grown in a dish. These two types of cells were stained with the DiD (red) and DiO (green), respectively. Figure 3.8 shows that the cells grew

together, but there is no overlapping suggesting interactions for spatial awareness.

Once we observed the mixing of the cells on a dish, we then wanted to know how these mixed cells would react when placed on a gel. In Figure 3.9, 25,000 of both ADSC and NHF cells were combined on a collagen I hydrogel in wells of a 96-well plate. ADSC and NHF cells were stained with Vybrant Cell Labeling Kit DiO (green) and DiD (red), respectively. DAPI was also applied to all cells as a counterstain for the nuclei. The resulting were concurrent with the previous study and the toroid showed major cellular intermingling. Notice that there are no yellow signals (where the fluorescence of the green ADSC and red NHF would be overlapping) This suggests that cells have some form of communication when mixed together that allow them to mix, migrate and form this toroid while keeping them from clumping together in an *in vivo*-like environment.

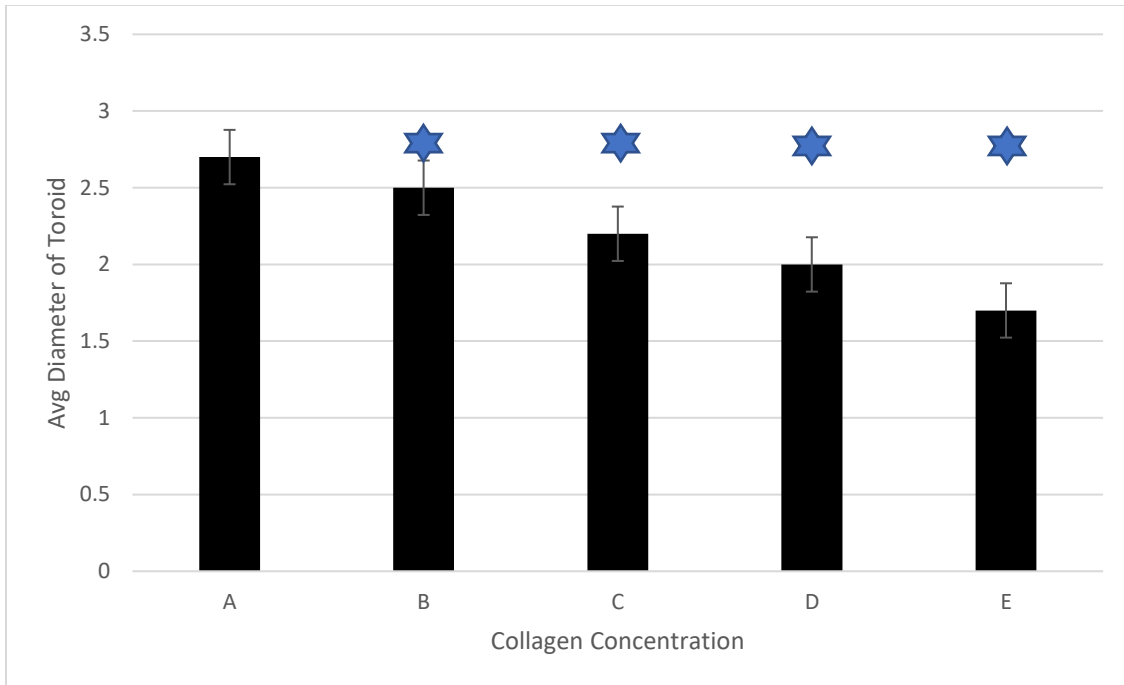


Figure 3.1 Bar Graph analysis of collagen concentration series. A collagen concentration series was performed using concentrations of A) 100% collagen I, B) 80:20 (collagen I: collagen III), C) 60:40, D) 40:60, and E) 100% collagen III. 50K NHF cells were placed on top of these gels and incubated for 24-hours at 37°C. Toroid diameter was measured and averaged. Bars B-E were all compared to Bar A (100% collagen I) and the stars show collagen I average. There is a correlating decrease in toroid diameter with increased collagen III concentration.

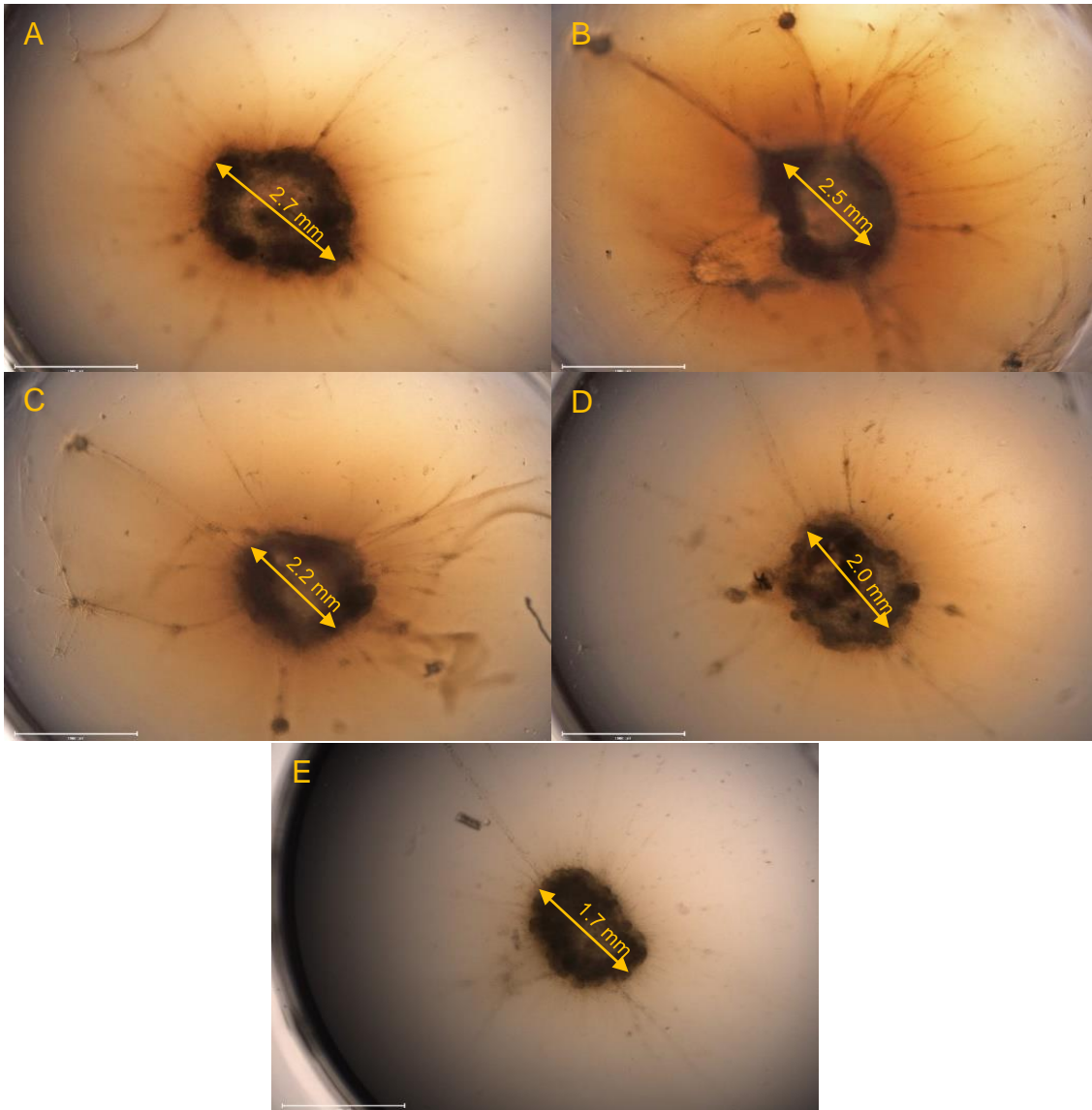


Figure 3.2 Collagen concentration series. Fifty-thousand cells were placed on each of the following concentration of collagen I and collagen III and allowed to incubate for 24-hours: A) 100% Collagen I. B) 80% Collagen I to 20% Collagen III. C) 60% Collagen I to 40% Collagen III. D) 40% Collagen I to 60% Collagen III. E) 100% Collagen III. When the diameters of the toroids were measured and averaged, we saw a 1 mm (37.04% difference between 100% collagen I (A) and 100% collagen III (E)). When statistically analyzed, a p-value of .000066 was calculated which was significant at $p < .01$.

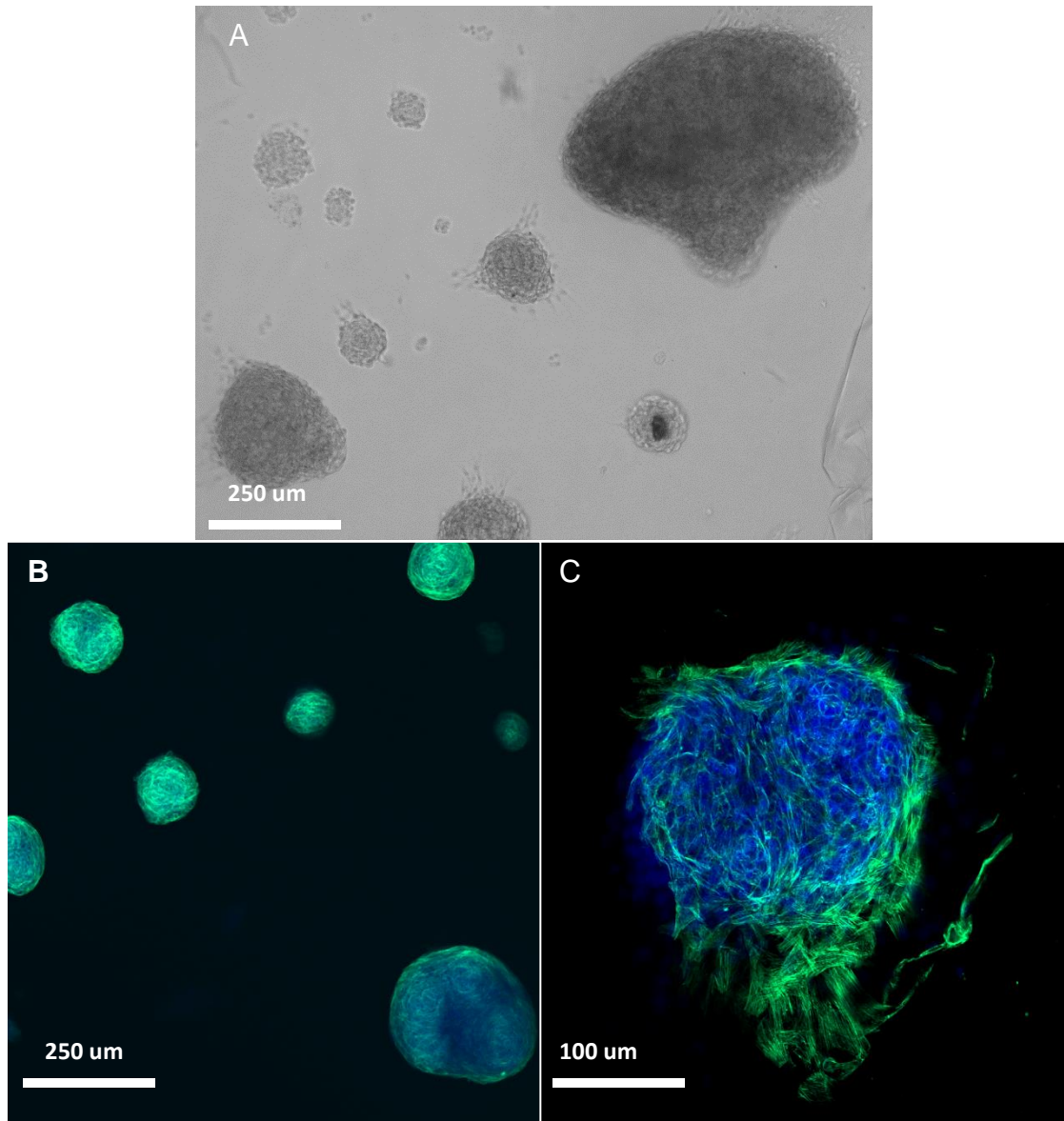


Figure 3.3 VitroGel™ 3D comparison to animal matrices. NHF cells stained with DAPI and Phalloidin 488. Images taken on the EVOS and Zeiss LSM 510. A) 20X bright-field image of the on top cells revealing cell clumps. B) 20X fluorescent image of the cellular clumps shown in A. C) 40X image of one cell clump showing nuclei bunched together with f-actin surrounding them.

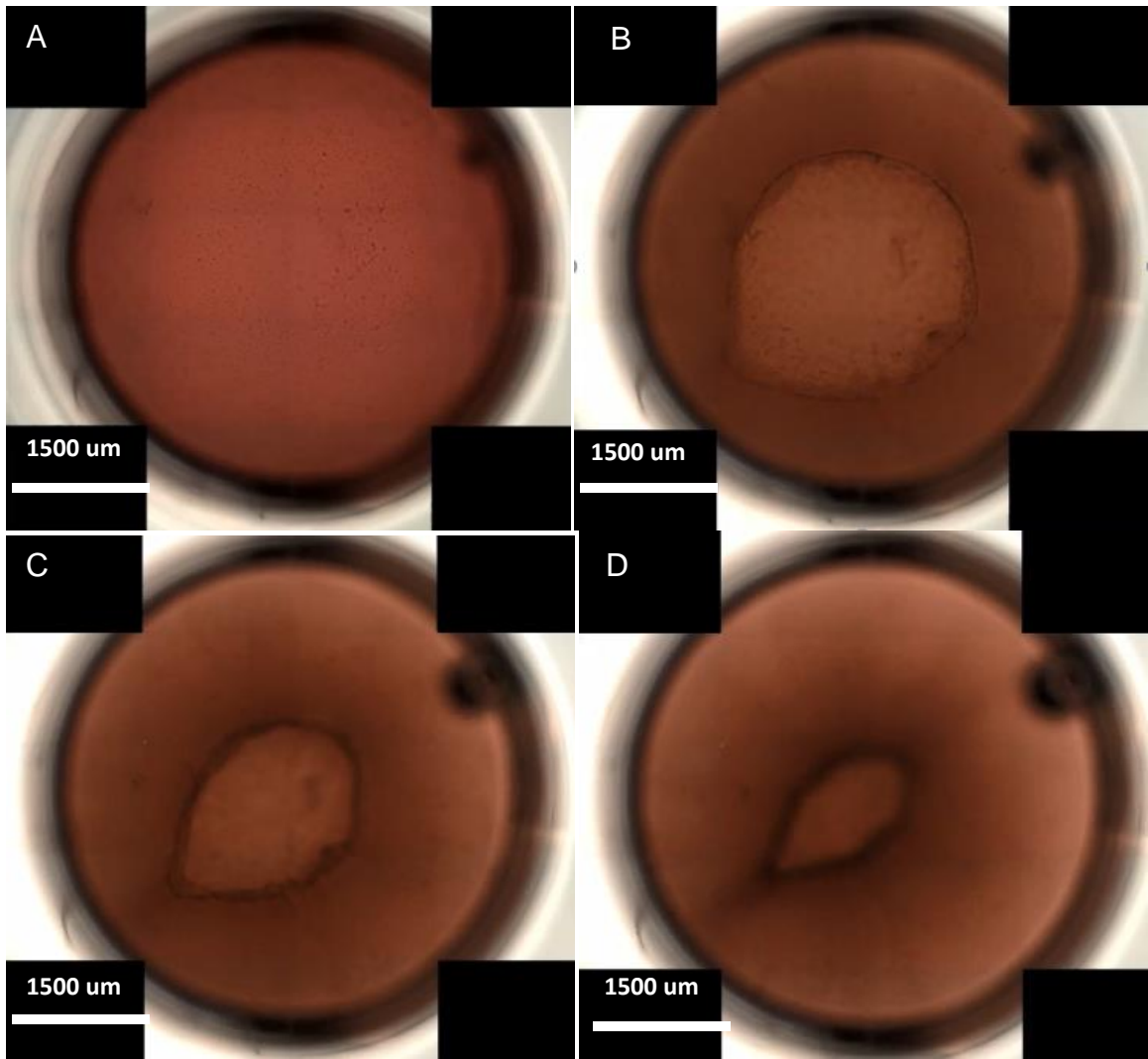


Figure 3.4 Bright-field time series. Images from a time series using collagen I hydrogel in a 96-well plate with 50,000 NHF cells show the formation of a toroid over a 24-hour period. Still-frame images were taken at 1, 10, 16, and 24-hours (A-D respectively) to generalize the movement seen in the time series. These images suggest that cells migrate from the outside of the well to form the toroid.

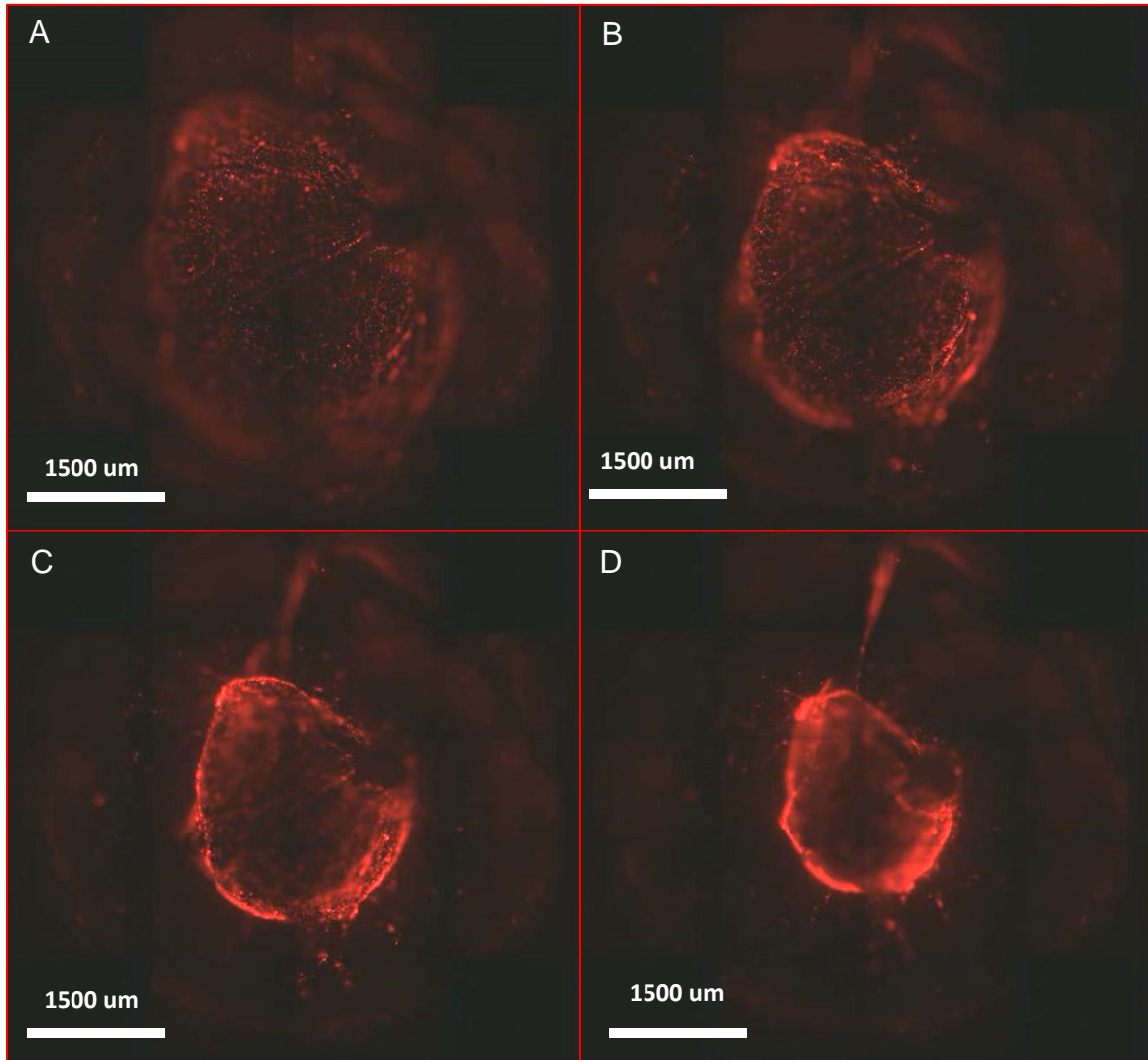


Figure 3.5 Fluorescent time series. Images from a time series using collagen I hydrogel in a 96-well plate with 50,000 NHF cells show the formation of a toroid over a 24-hour period. Cells were stained with Vybrant Cell Labeling DiD which emits in the far-red spectrum (665 nm). Still-frame images were taken at 1, 10, 16, and 24-hours (A-D respectively) to generalize the movement seen in the time series. While cells are easier to see in this time series when compared to the previous time series, we can only speculate from this that the cells are migrating from the outer portions of the gel to form a toroid.

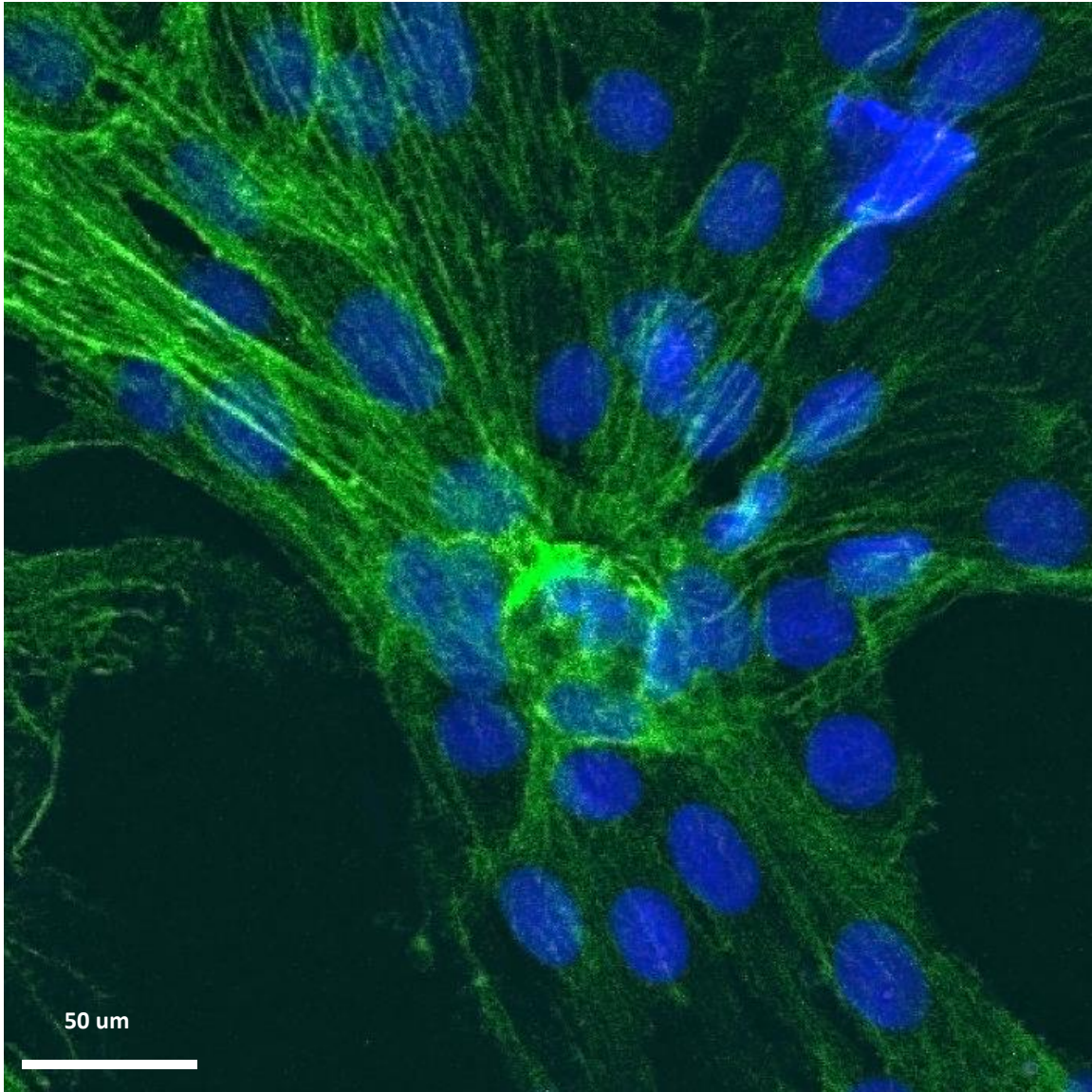


Figure 3.6 40X objective view of ITGB1 expression in ADSCs. Adipose-derived stem cells were transfected using the $\beta 1$ integrin expression vector and grown in a dish. Successful transfection could be confirmed due to the green fluorescence from the GFP tag. Image was collected on the Zeiss LSM 510 confocal microscope with the 40X objective. This image suggests that $\beta 1$ is expressed throughout the cell, mimicking the underlying f-actin. We can also observe that $\beta 1$ is formed in a perinuclear fashion.

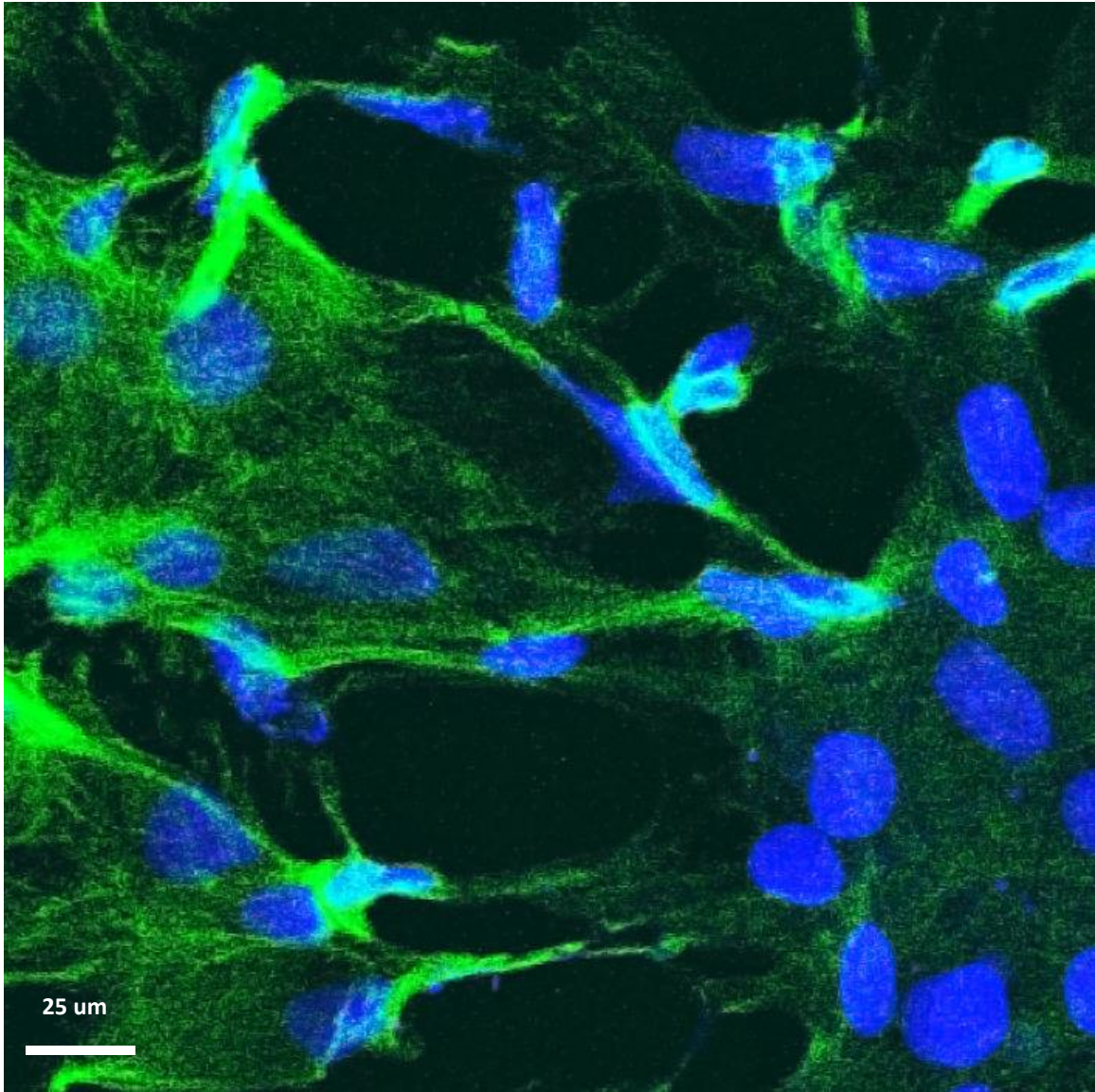


Figure 3.7 63X oil objective view of ITGB1 expression in ADSCs. Adipose-derived stem cells were transfected using the $\beta 1$ integrin expression vector and grown in a dish. Successful transfection could be confirmed due to the green fluorescence from the GFP tag. Image was collected on the Zeiss LSM 510 confocal microscope with the 63X oil objective. This image suggests that $\beta 1$ is expressed throughout the cell, mimicking the underlying f-actin. We can also observe that $\beta 1$ is formed in a perinuclear fashion.

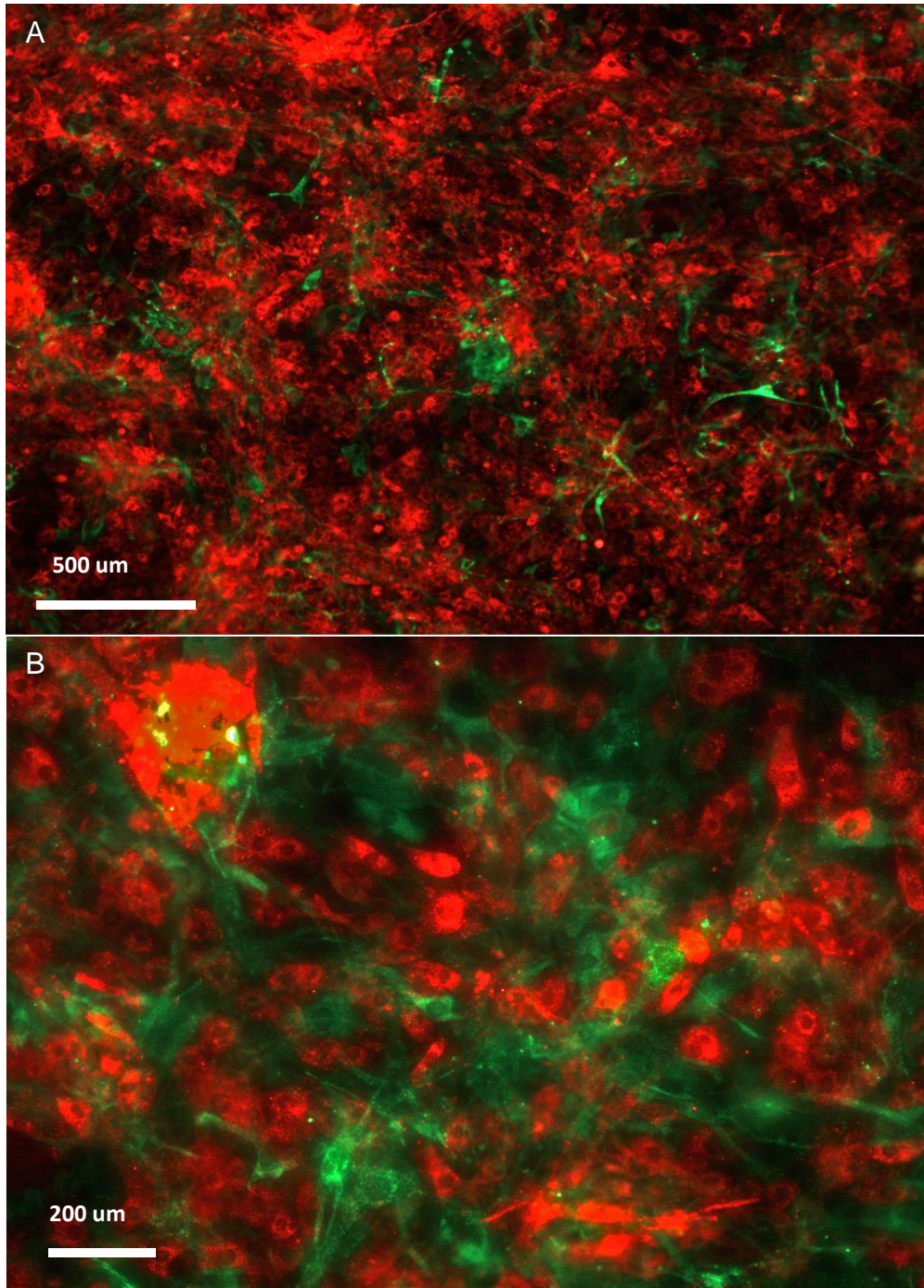


Figure 3.8 ADSC and BMSC mixed cells on a dish. ADSC (red) and BMSC (green) were mixed and plated on a dish. These images suggest that when the two cell types are mixed, they will mix together, but they will remain spatially segregated suggesting interaction between the two cell types as they grow together. A) 10X objective B) 20X objective.

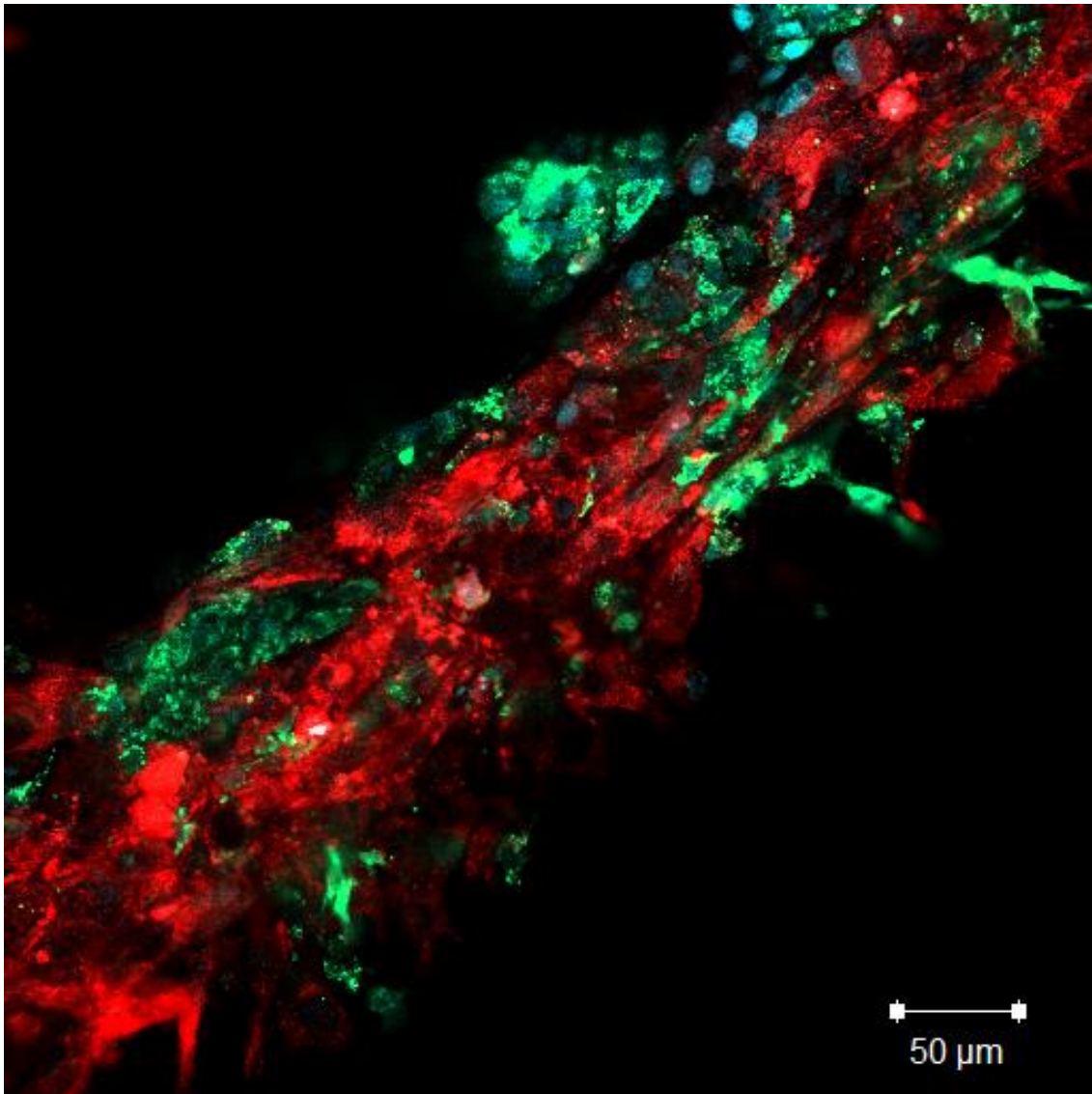


Figure 3.9 NHF and ADSC mixed cell toroid. Twenty-five thousand of both NHF (red- Vybrant DiD) and ADSC (green- Vybrant DiO) were placed on top of a collagen I hydrogel. DAPI is applied as a nuclear stain for all cells. This image shows that while the cells appear to be intermingling, there is no (yellow) signal produced when the red and green overlap. These results suggest that mixed cells will intermingle, migrate and form a toroid while maintaining their own space.

CHAPTER 4

DISCUSSION

The *objective* of this study was to observe and image cellular behavior when placed on top and mixed into the collagen hydrogels while studying cellular behavior when multiple cell types were mixed. We hypothesized that, when cells were mixed together, they would behave as if they were a single cell type rather than two distinct populations. While we chose collagen I hydrogels based on previous studies indicating that this type of hydrogel provides an acceptable and consistent extracellular matrix-like environment for cellular studies, this still needed to be tested for our experiments. The results from both the collagen concentration series and the VitroGel™ 3D non-animal model testing confirmed that collagen was superior to the carbohydrate bound matrix when it came to toroid formation. While the collagen III hydrogels produced toroids they were significantly smaller and more compact when compared to collagen I hydrogel which made imaging deeper and at a higher resolution more problematic.

The non-animal VitroGel™ 3D produced no toroids in any of the gels we tried. However, the cells were alive and did create interesting cell clumps. These clumps were similar to those shown in company literature (Powell, 2017). Even though this non-animal model did not work in forming toroids, there are other matrices to try. One such popular biomaterial we plan to examine is Polyethylene

Glycol or PEG gels. PEG has been used in various cell scaffold studies and is worth future integration (Bhaskar et al, 2018). The results from this study showed a decrease in toroid size as collagen III concentration increased thus supporting our claim that collagen I is an excellent hydrogel matrix when studying cellular interactions in an *in vivo*-like environment.

The first part of our experiment was to observe a single type of cells over a period of time to show their migration patterns. This was performed through a time series and timed fixation. The results from these studies supported our hypothesis that cells start to spread out within the well and migrate from the outside of the gel form the toroid. Both the bright-field and the fluorescent time series images suggest that these cells migrate over a 24-hour period. When observing the images, the migration of cells within the hydrogel is apparent. In the first hour, the cells cover the hydrogel and spread completely around the well. At hour twenty-four, however, the cells have migrated to form a toroid.

The results of the $\beta 1$ integrin study shows perinuclear expression of $\beta 1$ integrin throughout the cells almost mimicking the underlying f-actin. By using an expression vector, we were able to observe connections between cells and the ECM under fluorescence. In Figures 3.6 and 3.7, we can clearly see the $\beta 1$ integrin expression between the cells and the ECM.

The final study supports our hypothesis that when different cells are mixed together, they will interact and migrate as if they were a single cell population. In the NHF and ADSC combination toroid image, these cells are shown to have combined to create this toroid. When viewed closely, it can be seen that the red

NHF cells and the green ADSC cells are spatially separated but have still formed the toroid together.

The 10X and 20X images of the ADSC and BMSC mixed dish further supports our hypothesis by showing the interactions between the two stem cells. Notice in Figure 3.8, we can observe that the two cell types have mixed completely. Where there is a red ADSC, there is no green BMSC and vice versa. This is due to the cellular interactions that are occurring between the cells. This suggests that could be some form of communication between cells that allows them to be spatially aware of each other.

This study provided the evidence to support our claim that cells will interact and migrate together when combined with different cell types rather than growing in separate areas. This study has provided the means to observe and map specific cells and groups of cells as they migrate through a collagen hydrogel. Evidence has been provided that supports our tenet that collagen type I is useful for cellular studies and that cells will migrate and remodel their surrounding environment in a similar manner to their in vivo behavior.

CHAPTER 5

FUTURE DIRECTIONS

While numerous replicates were performed, additional experiments with other cell types are necessary to provide further evidence that would solidify and validate the data presented in this study. Expanding the study to include other cell types from differing sources would provide further insight into the cellular interaction and migration patterns when combined in hostile microenvironments.

The impact of differing hydrogel matrices on cellular behavior should be explored further. In doing so, single cell types and combinations of cells should be placed on other biomaterials such as Polyethylene Glycol (PEG), Poly-Lactic-co-Glycolic Acid (PLGA), and collagen V.

The use of the ITGB1 expression vectors, as well as other targeted vectors, should be expanded in future studies. Viewing β 1 integrin transfected cells in conjunction with other labeled cells could provide images of these mixed cells interacting with one another. Additional directions may be to replace the GFP tag in the ITGB1 vector with another fluorescent tag that emits in a different spectrum so that two different cell types can be transformed and viewed to overexpress ITGB1. This might give insight to the directions of different cell-to-ECM connections when cells are mixed together.

Viewing these studies on larger gels may also provide a different view of the results. By forming gels in a 24-well plate, toroids would be approximately four times larger than in a 96-well plate. This could allow for a better observation of the cellular interactions when combined to form a toroid.

REFERENCES

- Ali Khawar I, Park JK, Jung ES, Lee MA, Chang S, Kuh HJ. (2018). Three Dimensional Mixed-Cell Spheroids Mimic Stroma-Mediated Chemoresistance and Invasive Migration in hepatocellular carcinoma. *Neoplasia*. 20: 800-812.
- Antoine EE, Vlachos PP, Rylander MN. (2015). Tunable Collagen I Hydrogels for Engineered Physiological Tissue Micro-Environments. *PLoS ONE*. 10(3): e0122500.
- Athanasopoulos T, Munye MM, Yanez-Munoz J. (2017). Nonintegrating Gene Therapy Vectors. *Hematol Oncol Clin N Am*. 31: 753-770.
- Bhaskar B, Owen R, Bahmaee H, Wally Z, Sreenivasa Rao P, Reilly GC. 2018. Composite porous scaffold of PEG/PLA support improved bone matrix deposition in vitro compares to PLA-only scaffolds. *J Biomed Res A*. 106(5): 1334-1340.
- Dey A and Reddy G. (2017). Toroidal Condensates by Semiflexible Polymer Chains: Insights into Nucleation, Growth and Packing Defects. *J Phys Chem B*. 121: 9291-9301.
- Escobar-Aguirre S, Arancibia A, Escorza A, Bravo C, Andres ME, Zamorano P, Martinez V. (2019). Development of a Bicistronic Vector for the Expression of a CRISPR/Cas9-mCherry System in Fish Cell Lines. *Cell's*. 8(1), 75.
- Fan C and Wang D. (2017) Macroporous Hydrogel Scaffolds for Three-Dimensional Cell Culture and Tissue Engineering. *Tissue Engineering B*. 23(5): 451-461.
- Fleming PA, Argraves WS, Gentile C, Neagu A, Forgacs G, Drake CJ. (2010). Fusion of uniluminal vascular spheroids: a model for assembly of blood vessels. *Dev Dyn*. 239(2): 398-406.
- Gourdie RG, Myers TA, McFadden A, Li Y, Potts JD. (2012). Self-Organizing Tissue-Engineered Constructs in Collagen Hydrogels. *Microsc Microanal*. 18: 99.
- Gupta M, Srivastava YK, Singh R. (2018). A Toroidal Metamaterial Switch. *Adv Mater*. 30: 1704845.

- Hesse E, Hefferan TE, Tarara JE, Haasper C, Meller R, Krettek C, Lu L, Yaszemski MJ. (2010). Collagen type I hydrogel allows migration, proliferation and osteogenic differentiation of rat bone marrow stromal cells. *J Biomed Mater Res A*. 94(2): 442-449.
- Iervolino A, De La Motte LR, Petrillo F, Prosperi F, Alvino FM, Schiano G, Perna AF, Di Matteo D, De Felice M, Capasso G, et al. (2018). Integrin Beta 1 Is Crucial for Urinary Concentrating Ability and Renal Medulla Architecture in Adult Mice. *Front. Physiol.* 9: 1273.
- Lee SH, Shim KY, Kim B, Sung JH. (2017). Hydrogel-Based Three-Dimensional Cell Culture for Organ-on-a-Chip Applications. *Biotechnol Prog.* 33(3): 580-589.
- Liu Z, Du S, Cui A, Li Z, Fan Y, Chen S, Li W, Li J, Gu C. (2017). High-Quality-Factor Mid-Infrared Toroidal Excitation in Folded 3D Metamaterials. *Adv Mater.* 29: 1606298.
- Livoti CM and Morgan JR. (2010). Self-Assembly and Tissue Fusion of Toroid-Shaped Minimal Building Units. *Tissue Engineering A*. 16(6): 2051- 2061.
- Mao X, Cheng R, Zhang H, Bae J, Cheng L, Zhang L, Deng L, Cui W, Zhang Y, Santos H, et al. (2019). Self-Healing and Injectable Hydrogel for Matching Skin Flap Regeneration. *Adv Sci.* 6: 1801555.
- Masuda T, Takei N, Nakano T, Anada T, Suzuki O, Arai F. (2012). A microfabricated platform to form three-dimensional toroidal multicellular aggregate. *Biomed Microdevices.* 14: 1085-1093.
- Menon V, Eberth JF, Junor L, Potts AJ, Balhaj M, Dipette DJ, Jenkins MW, Potts JD. 2018. Removing vessel constriction on the embryonic heart results in changes in valve gene expression, morphology, and hemodynamics. *Dev Dyn.* 247(3): 531-541.
- Mir TA and Nakamura M. (2017). Three-Dimensional Bioprinting: Toward the Era of Manufacturing Human Organs as Spare Parts for Healthcare and Medicine. *Tissue Engineering B*. 23(3): 245-256.
- Naahidi S, Jafari M, Logan M, Wang Y, Yuan Y, Bae H, Dixon B, Chen P. (2017). Biocompatibility of hydrogel-based scaffolds for tissue engineering applications. *Biotechnology Advances.* 35: 530-544.
- Nirwal S, Kulkarni DS, Sharma A, Rao DN, Nair DT. (2018). Mechanism of formation of a toroid around DNA by the mismatch sensor protein. *Nucleic Acids Research.* 46(1): 256-266.
- Oliveira JM, Carvalho L, Silva-Correia J, Vieira S, Majchrzak M, Lukomska B, Stanaszek L, Strymecka P, Malysz-Cymborska I, Golubczyk D, et al.

- (2018). Hydrogel-based scaffolds to support intrathecal stem cell transplantation as a gateway to the spinal cord: clinical needs, biomaterials, and imaging technologies. *Npj Regenerative Medicine*. 3: 8.
- Paddock SW. (2000). Principles and Practices of Laser Scanning Confocal Microscopy. *Molecular Biotechnology*. 16: 127-149.
- Piccinini F, Tesei A, Zanoni M, Bevilacqua A. (2017). ReViMS: Software tool for estimating the volumes of 3-D multicellular spheroids imaged using a light sheet fluorescence microscope. *BioTechniques*. 63(5): 227-229.
- Potts JD and Runyan RB. 1989. Epithelial-Mesenchymal Transformation in the Embryonic Heart Can Be Mediated, In Part, By Transforming Growth Factor-B. *Dev Biol*. 134:392-401.
- Powell K. (2017). Adding depth to cell culture. *Science*. 4: 96-98.
- Quekett J. (1848). *A Practical Treatise on the use of the Microscope*. 306.
- Renz M. (2013). Fluorescence Microscopy- A Historical and Technical Perspective. *Cytometry*. 83A: 767-779.
- Runyan RB, Potts JD, Weeks DL. 1992. TGFB-3 Mediated Tissue Interaction During Embryonic Heart Development. *Mol Reprod and Dev*. 32:152-159.
- Sato K, Choyke PL, Hisataka K. (2016). Selective cell Elimination from Mixed 3D Culture Using a Near Infrared Photoimmunotherapy Technique. *J Vis Exp*. 109, e53633.
- Short AR, Czeisler C, Stocker B, Cole S, Otero JJ, Winter JO. (2017). Imaging Cell-Matrix Interactions in Three-Dimensional Collagen Hydrogel Culture Systems. *Macromol Biosci*. 17(6):1-17.
- Sinha R, Verdonschot N, Koopman B, Rouwkema J. (2017). Tuning Cell and Tissue Development by Combining Multiple Mechanical Signals. *Tissue Engineering B*. 23(5): 494-504.
- Stanton MM, Samitier J, Sanchez S. (2015). Bioprinting of 3D Hydrogels. *Lab Chip*. 15: 3111-3115.
- Stoien JD and Wang RJ. (1974). Effect of Near-Ultraviolet and Visible Light on Mammalian Cells in Culture II-Formation of Toxic Photoproducts in Tissue Culture Medium by Blacklight. *Proc Nat Acad Sci USA*. 71(10): 3961-3965.
- Sun Q, Zhou C, Ma R, Huo Q, Huang H, Hao J, Liu H, Shi R, Liu B. (2018). Prognostic value of increased integrin-beta 1 expression in solid cancers: a meta-analysis. *Onco Targets and Therapy*. 11:1787-1799.

- Uluc K, Kujoth GC, Baskaya MK. (2009). Operating microscopes: past, present, and future. *Neurosurg Focus*. 27(3): E4.
- Vadivelu RK, Kamble H, Munaz A, Nguyen N. (2017). Liquid Marble as Bioreactor for Engineering Three-Dimensional Toroid Tissues. *Sci Reports*. 7: 12388.
- Van Duinen V, Trietsch SJ, Joore J, Vulto P, Hankemeier T. (2015). Microfluidic 3D cell culture: from tools to tissue models. *Current Opinion in Biotechnology*. 35: 118-126.
- Van Gaalen SM, Kruyt MC, Geuze RE, de Bruijn JD, Alblas J, Dhert WJA. (2010). Use of Fluorochrome Labels in *In Vivo* Bone Tissue Engineering Research. *Tissue Engineering*. 16(2): 209-217.
- Vu LT, Jain G, Veres BD, Rajagopalan P. (2015). Cell Migration on Planar and Three-Dimensional Matrices: A Hydrogel-Based Perspective. *Tissue Engineering B*. 21(1): 67-74.
- Wadkin LE, Orozco-Fuentes S, Neganova I, Swan G, Laude A, Lako M, Shukurov A, Parker NG. (2018). Correlated random walks of human embryonic stem cells *in vitro*. *Phys Bio*. 15: e056006.
- Yang C, Qiu L, Xu Z. (2011). Specific Gene Silencing Using RNAi in Cell Culture. *Methods Mol Biol*. 793: 457-477.
- Zhang W, Zhang M, Liu L, Jin D, Wang P, Hu J. (2018). MicroRNA-183-5p Inhibits Aggressiveness of Cervical Cancer Cells by Targeting Integrin Subunit Beta 1 (ITGB1). *Med Sci Monit*. 24:7137-7145.